Giant magnetic domain-wall resistance in phase-separated manganite films

L. Granja,[1] L. E. Hueso,[2,a)] J. L. Prieto,[2,b)] P. Levy,[1] and N. D. Mathur[2,c)]
[1]*Departamento de Materia Condensada, Gerencia de Investigación y Aplicaciones, Comisión Nacional de Energía Atómica, General Paz 1499 (1650), San Martín, Buenos Aires, Argentina*
[2]*Department of Materials Science, University of Cambridge, Pembroke Street, Cambridge CB2 3QZ, United Kingdom*

(Received 12 August 2010; accepted 28 November 2010; published online 20 December 2010)

The top and bottom electrodes of the ferromagnetic manganite $La_{0.7}Ca_{0.3}MnO_3$ may be magnetically decoupled by a $La_{0.59}Ca_{0.41}MnO_3$ interlayer in which ferromagnetic and paramagnetic phases coexist. In mesas fabricated from these trilayer films, in-plane magnetic domain walls associated with the antiparallel magnetic electrode configuration show a giant resistance-area product $>10^{-10}$ Ω m^2. This is almost two orders of magnitude larger than our devices with interlayer composition $La_{0.6}Ca_{0.4}MnO_3$ [C. Israel *et al.*, Phys. Rev. B **78**, 054409 (2008)] where phase separation is less extreme. High-field treatments modify the ferromagnetic phase fraction of the interlayer. © *2010 American Institute of Physics*. [doi:10.1063/1.3527942]

In the mid-1990s, the pseudocubic perovskite manganites became well known for colossal magnetoresistance where magnetic fields of several tesla align Mn core spins and reduce electrical resistivity by many orders of magnitude.[1] Low-field magnetoresistance (LFMR) effects in which millitesla fields are sufficient to align ferromagnetic domains across structural discontinuities such as grain boundaries[2–4] or tunnel barriers[5,6] were also observed. More recently, interest in the manganites has tended to focus on phase-separation phenomena where ferromagnetic metallic (FMM) phases coexist over a wide range of length scales with highly insulating charge-ordered and/or paramagnetic phases.[7,8]

Mathur and Littlewood[9] proposed that magnetic domain walls could be highly resistive due to phase separation at wall centers, and so devices designed to trap domain walls should show a pronounced LFMR. LFMR has been observed in lateral domain-wall devices based on single films,[10–12] but reproducibility is poor for three reasons. First, the micromagnetics of complex oxides is challenging. Second, patterned tracks have a large surface-area-to-volume ratio, which may introduce artifacts, especially at milled track edges. Third, nanoconstrictions designed to trap domain walls experience relatively high current densities.

We have previously achieved LFMR via domain walls in all-manganite epitaxial trilayer films[13] and devices.[14] Top and bottom FMM electrodes of $La_{0.7}Ca_{0.3}MnO_3$ (LCMO30) were magnetically decoupled by a phase-separated interlayer whose FMM regions support domain walls. This interlayer had a larger Ca:La ratio than the electrodes, placing it near the edge of the FMM phase field in the thin-film phase diagram.[15] Current-in-the-plane (CIP) measurements of unpatterned trilayers,[13] and current-out-of-the-plane (CPP) measurements of mesas[14] were highly reproducible because the three problems discussed above for single-layer devices are avoided. First, electrode magnetizations switch independently because the phase-separated interlayer is a weak magnetic link. Second, transport though buried interlayer domain walls is not corrupted by surface effects. Third, heating effects are unlikely as the active areas are large, unlike nanoconstrictions in thin films.

Our previous CPP measurements of 5×5 μm^2 mesas defined from LCMO30/LCMO40/LCMO30 trilayers established a domain-wall resistance-area (RA) product 3×10^{-12} Ω m$^2 \leq RA \leq 6.3\times10^{-12}$ Ω m^2.[14] Here, effective area A is 20%–42% of the mesa area to take into account the areal fraction occupied by three-dimensional FMM pathways in LCMO40.[14] A 1% change in doping from LCMO40 to LCMO41 is known to be reproducible and significant,[15] but our previous measurements of domain walls using LCMO41 as the interlayer composition in CIP trilayers could not return values of RA.[13] Here, CPP measurements of trilayers reveal that RA is increased almost two orders of magnitude when the LCMO40 interlayer[14] is replaced with LCMO41. We also show that device resistance may be tuned using large magnetic fields to increase the effective area of FMM pathways in the LCMO41 interlayer.

Three manganite trilayers of LCMO30 (20 nm)/LCMO41 (δ nm)/LCMO30 (50 nm)//NGO with δ=10, 20, and 40, covered by a 50 nm *in situ* gold cap to improve contact resistance, were prepared as described previously[14] using pulsed laser deposition. Epitaxial growth and film thicknesses were confirmed by x-ray diffraction. CPP devices with square 5×5 μm^2 mesas were defined from each trilayer as described previously[14] using optical lithography, Ar ion milling, and sputtering for silica insulation and gold contacts. The devices are reminiscent of magnetic tunnel junctions,[6] but the electrodes are separated by a phase-separated interlayer rather than a tunnel barrier. One side of each mesa, and the long axis of each bottom electrode, were parallel to the orthorhombic [100] magnetic easy axis of the LCMO30 electrodes.[16]

Magnetic measurements of the unpatterned trilayer films were performed using a vibrating sample magnetometer. Four-terminal electrical measurements of the CPP devices were performed as a function of temperature (20–300 K) and magnetic field parallel to [100] in either a closed-cycle He cryostat (150 μA, $\pm$0.5 T) or a Quantum Design Physical

a)Present address: CIC nanoGUNE Consolider, Tolosa Hiribidea 76, E-20018 Donostia, San Sebastian and IKERBASQUE, Basque Foundation for Science, E-48011 Bilbao, Spain.
b)Present address: Intituto de Sistemas Optoelectrónicos y Microtecnología (ISOM), Universidad Politécnica de Madrid (UPM), Avda. Complutense s/n, Madrid 28040, Spain.
c)Author to whom correspondence should be addressed. Electronic mail: ndm12@cam.ac.uk.

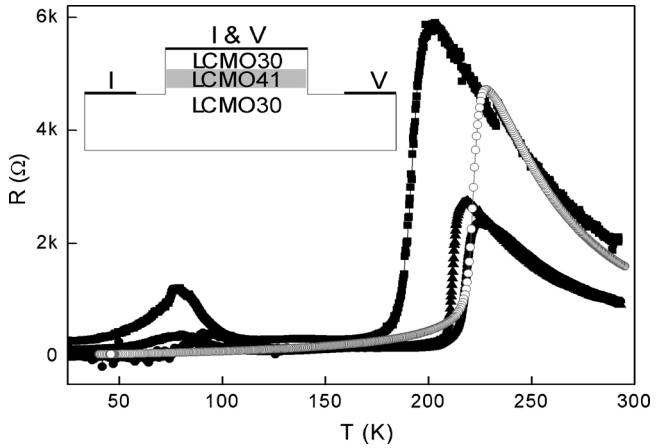

FIG. 1. Resistance R vs temperature T for three CPP devices with δ=10 (▲), 20 (■), and 40 (●) nm. Four-terminal CIP measurements of an unpatterned trilayer with δ=20 nm (○) are also shown. Inset: schematic device geometry showing contact pads (thick lines) for voltage V and current I terminals.

Property Measurement System (10 μA, ±9 T). All current-voltage characteristics were linear, and our use of small currents avoids heating. As with standard tunnel junctions, we performed three-terminal measurements since the small top contact must be shared between current and voltage leads.

Figure 1 shows resistance R versus temperature T for the three CPP trilayer devices. Each displays a metal-insulator transition near 200 K due to the LCMO41 interlayer. Above this temperature, the interlayer dominates device resistance, masking the ~260 K metal-insulator transition[16] of the LCMO30 electrodes. The feature near 80 K arises due to a metal-insulator transition in degraded material directly under the top contact,[17] and is therefore absent in four-terminal CIP measurements of an unpatterned trilayer, as shown for δ =20 nm in Fig. 1. All subsequent data that we present were measured below this temperature.

Figure 2 shows magnetization M versus applied magnetic field $\mu_0 H=B$ at 50 K for three codeposited and unpatterned trilayer films. The switching of the 50 nm bottom electrodes produces the expected[13] sharp jumps in all three films. The switching of the 20 nm top electrodes produces correspondingly smaller jumps, but for δ=40 nm the jump is unexpectedly small. We see that the LCMO41 interlayer magnetically decouples the top and bottom electrodes either everywhere (δ=10 and 20 nm) or at least somewhere (δ =40 nm) in our large-area samples. Increases in trilayer magnetization away from jump fields arise from the interlayer, primarily due to FMM domain alignment.[13]

Figure 3 shows resistance R versus $\mu_0 H=B$ at 25 K for the three devices. Each device shows a two-state LFMR associated with top and bottom electrode magnetizations switching between parallel and antiparallel configurations. This electrical switching was highly reproducible between field sweeps and cooling runs, but absolute values of R varied from run to run due to variations in top-electrode contact resistance. Jump magnitude $RA > 10^{-10}$ Ω m^2 was found to decrease with increasing δ (Fig. 3, inset) but is almost two orders of magnitude larger than our previous figure[14] of $RA > 10^{-12}$ Ω m^2 for an LCMO40 interlayer with δ=20 nm [effective transport area A was calculated using FMM volume fractions 38% (LCMO41)[15] and 42% (LCMO40)[14]].

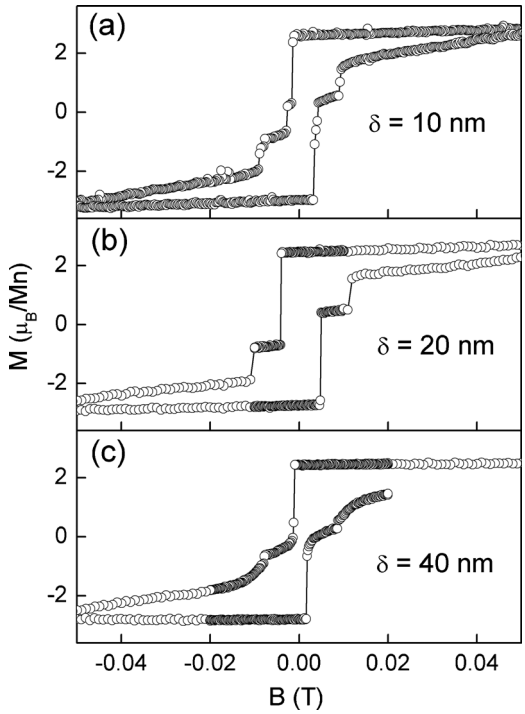

FIG. 2. Magnetization M vs applied magnetic field $\mu_0 H=B$ at 50 K for the three unpatterned trilayer films cut to 4×4 mm^2.

Figure 4 shows high-field magnetoresistance (HFMR) versus $\mu_0 H=B$ at 25 K for the three devices. The application of several tesla produces a large virgin HFMR of around −80% due to an increase in interlayer FMM volume fraction; cf. memory effects in other phase-separated manganites such as $La_{0.5}Ca_{0.5}MnO_3$.[18] Figure 4 shows that subsequent high-field cycling produces a small hysteresis associated with interlayer FMM volume fraction. We also report here a similar HFMR ~ −60% (Fig. 4) for our previous CPP device[14] with an LCMO40 interlayer. The 33% increase in HFMR strength on replacing LCMO40 with LCMO41 is attributed to the decrease in FMM volume fraction,[15] but no formal link can be established as the fraction of isolated FMM regions is unknown.

After reducing the resistance of our δ=10 nm device at 25 K by applying and removing $\mu_0 H$=9 T, we were able to

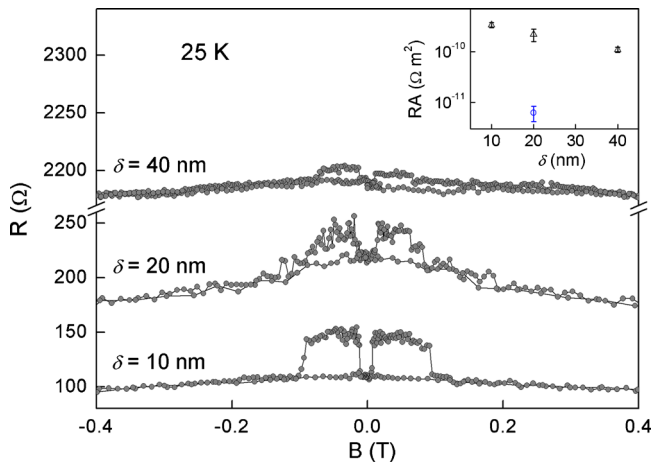

FIG. 3. (Color online) Resistance R vs $\mu_0 H=B$ at 25 K after zero-field cooling, for the three CPP devices. The inset shows low-field switching jump RA vs δ for these devices (△) and our previous CPP device with an LCMO40 interlayer (○).

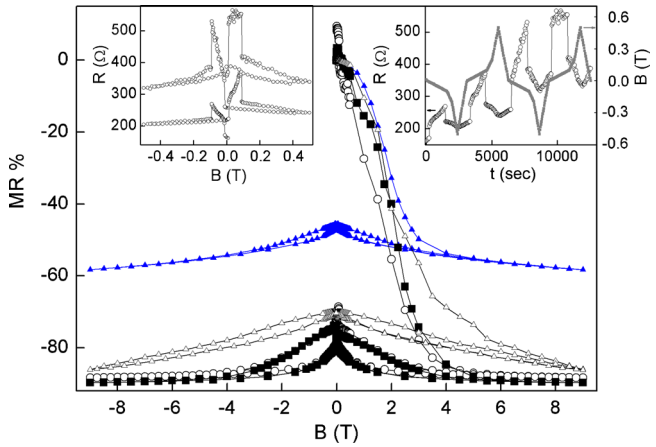

FIG. 4. (Color online) Magnetoresistance MR in $B=\pm 9$ T, after zero-field cooling to 25 K and then cycling in a small field ($\mu_0 H=\pm 0.5$ T) to remove magnetic domains, for the three CPP devices with LCMO41 interlayers of thicknesses $\delta=10$ nm (○), 20 nm (■), and 40 nm (△). Equivalent data are also shown for the CPP device of Ref. 14, which has an LCMO40 interlayer of thickness $\delta=20$ nm (▲). Left inset: LFMR for the $\delta=10$ nm device at 25 K after having applied and removed $\mu_0 H=9$ T. The right inset shows how these data were collected over time t.

observe a two-state LFMR associated with parallel and antiparallel electrode configurations (left inset, Fig. 4). These data contain a time dependence that we plot explicitly (right inset, Fig. 4) to reveal that device resistance tends to increase with time for a given electrode configuration. This increase arises because the field-enhanced FMM volume fraction of the interlayer reduces over time back toward equilibrium.[18]

The phenomenon of the LFMR in our CPP devices exploits both phase separation[15] and CPP percolation in our LCMO41 interlayer material. The presence of the PM phase renders LCMO41 a weak magnetic link that decouples the FMM electrodes (Fig. 2) without incurring significant damage during device processing.[10–12] The percolating FMM phase permits spin-coherent transport between the FMM LCMO30 electrodes. Parallel and antiparallel electrode magnetizations correspond to low and high states of resistance (Figs. 3 and 4, insets) because the antiparallel configuration forces resistive in-plane magnetic domain walls to form in the FMM pathways of the interlayer.

These magnetic domain walls are resistive at least in part because they are constrained[19] within the three-dimensional filamentary FMM pathways that we assume to exist as they do in LCMO40.[14] Our thickest interlayer is comparable with the natural domain-wall width (38 ± 10 nm) of the FMM phase of manganites,[20] and the small increase in RA with decreasing δ could arise because domain walls in the thinner interlayers are vertically constrained. Note that the variation in RA with δ cannot be due to anisotropic magnetoresistance in our simple geometry.

Our work supports the idea that phase separation dramatically increases the resistance of magnetic domain walls in manganites.[9] We have increased RA almost two orders of magnitude by replacing the LCMO40 interlayer with LCMO41 in our CPP devices. LCMO41 lies nearer to the thin-film phase boundary[15] than LCMO40 and therefore shows a more extreme tendency to phase separate. Our domain-wall resistance-area product of $>10^{-10}$ Ω m^2 is large compared with other manganites (10^{-15}–10^{-11} Ω m^2)[10–12,21] and elemental ferromagnets such as cobalt (10^{-19} Ω m^2).[22]

Our work also demonstrates how phase separation in the LCMO41 interlayers may be exploited to achieve HFMR effects. The ability to achieve LFMR after varying device resistance in HFMR experiments is reminiscent of four-state memory devices.[23] By applying large magnetic fields, it is possible to control the FMM volume fraction of the interlayer and thus access different absolute levels of device resistance. The subsequent LFMR is large with respect to the changes that arise while the FMM volume fraction of the interlayer reduces back toward equilibrium. Our demonstration of LFMR and HFMR in buried FMM pathways represents an attractive basis for future studies in which both phase separation and spintronics are explored and exploited in manganites.

We thank L. Fraigi *et al.* at the INTI for the technical support. This work was funded by the EU Alßan programme (L.G., Grant No. E03D18900AR, the Marie Curie Fellowships (L.E.H., Contract No. HPMF-CT-2002-01851 and J.L.P., Contract No. MCFI-2000-01343) and the EPSRC (U.K.). L.G. and P.L. are members of CONICET.

[1] S. Jin, T. H. Tiefel, M. McCormack, R. A. Fastnacht, R. Ramesh, and L. H. Chen, Science **264**, 413 (1994).
[2] H. Y. Hwang, S.-W. Cheong, N. P. Ong, and B. Batlogg, Phys. Rev. Lett. **77**, 2041 (1996).
[3] A. Gupta, G. Q. Gong, G. Xiao, P. R. Duncombe, P. Lecoeur, P. Trouilloud, Y. Y. Wang, V. P. Dravid, and J. Z. Sun, Phys. Rev. B **54**, R15629 (1996).
[4] N. D. Mathur, G. Burnell, S. P. Isaac, T. J. Jackson, B.-S. Teo, J. L. MacManus-Driscoll, L. F. Cohen, J. E. Evetts, and M. G. Blamire, Nature (London) **387**, 266 (1997).
[5] J. Z. Sun, W. J. Gallagher, P. R. Duncombe, L. Krusin-Elbaum, R. A. Altman, A. Gupta, Y. Lu, G. Q. Gong, and G. Xiao, Appl. Phys. Lett. **69**, 3266 (1996).
[6] M.-H. Jo, N. D. Mathur, N. K. Todd, and M. G. Blamire, Phys. Rev. B **61**, R14905 (2000).
[7] N. Mathur and P. Littlewood, Phys. Today **56**(1), 25 (2003).
[8] G. Singh-Bhalla, S. Selcuk, T. Dhakal, A. Biswas, and A. F. Hebard, Phys. Rev. Lett. **102**, 077205 (2009).
[9] N. D. Mathur and P. B. Littlewood, Solid State Commun. **119**, 271 (2001).
[10] N. D. Mathur, P. B. Littlewood, N. K. Todd, S. P. Isaac, B. S. Teo, D. J. Kang, E. J. Tarte, Z. H. Barber, J. E. Evetts, and M. G. Blamire, J. Appl. Phys. **86**, 6287 (1999).
[11] J. Wolfman, A. M. Haghiri-Gosnet, B. Raveau, C. Vieu, E. Cambril, A. Cornette, and H. Launois, J. Appl. Phys. **89**, 6955 (2001).
[12] T. Arnal, A. V. Khvalkovskii, M. Bibes, B. Mercey, P. Lecoeur, and A. M. Haghiri-Gosnet, Phys. Rev. B **75**, 220409(R) (2007).
[13] L. E. Hueso, L. Granja, P. Levy, and N. D. Mathur, J. Appl. Phys. **100**, 023903 (2006).
[14] C. Israel, L. Granja, T. M. Chuang, L. E. Hueso, D. Sánchez, J. L. Prieto, P. Levy, A. de Lozanne, and N. D. Mathur, Phys. Rev. B **78**, 054409 (2008).
[15] D. Sánchez, L. E. Hueso, L. Granja, P. Levy, and N. D. Mathur, Appl. Phys. Lett. **89**, 142509 (2006).
[16] N. D. Mathur, M. H. Jo, J. E. Evetts, and M. G. Blamire, J. Appl. Phys. **89**, 3388 (2001).
[17] L. Granja, L. E. Hueso, M. Quintero, P. Levy, and N. D. Mathur, Physica B **398**, 235 (2007).
[18] P. Levy, F. Parisi, L. Granja, E. Indelicato, and G. Polla, Phys. Rev. Lett. **89**, 137001 (2002).
[19] P. Bruno, Phys. Rev. Lett. **83**, 2425 (1999).
[20] S. J. Lloyd, N. D. Mathur, J. C. Loudon, and P. A. Midgley, Phys. Rev. B **64**, 172407 (2001).
[21] Y. Wu, Y. Suzuki, U. Rudiger, J. Yu, A. D. Kent, T. K. Nath, and C. B. Eom, Appl. Phys. Lett. **75**, 2295 (1999).
[22] U. Rüdiger, J. Yu, L. Thomas, S. S. P. Parkin, and A. D. Kent, Phys. Rev. B **59**, 11914 (1999).
[23] M. Gajek, M. Bibes, S. Fusil, K. Bouzehouane, J. Fontcuberta, A. Barthélémy, and A. Fert, Nature Mater. **6**, 296 (2007).